The maturing of high contrast imaging and starlight suppression techniques for future NASA exoplanet characterization missions

Daniel R. Coulter*, David B. Gallagher, Nicholas Siegler, Stuart Shaklan , Karl Stapelfeldt , Wesley A. Traub
Jet Propulsion Laboratory, California Institute of Technology,
4800 Oak Grove Drive, Pasadena, CA, USA, 91109-8099

ABSTRACT

Over 3000 exoplanets and hundreds of exoplanetary systems have been detected to date and we are now rapidly moving toward an era where the focus is shifting from detection to direct imaging and spectroscopic characterization of these new worlds and their atmospheres. NASA is currently studying several exoplanet characterization mission concepts for the 2020 Decadal Survey ranging from probe class to flagships. Detailed and comprehensive exoplanet characterization, particularly of exo-Earths, leading to assessment of habitability, or indeed detection of life, will require significant advances beyond the current state-of-the-art in high contrast imaging and starlight suppression techniques which utilize specially shaped precision optical elements to block the light from the parent star while controlling scattering and diffraction thus revealing and enabling spectroscopic study of the orbiting exoplanets in reflected light. In this paper we describe the two primary high contrast starlight suppression techniques currently being pursued by NASA: 1) coronagraphs (including several design variations) and 2) free-flying starshades. These techniques are rapidly moving from the technology development phase to the design and engineering phase and we discuss the prospects and projected performance for future exoplanet characterization missions utilizing these techniques coupled with large aperture telescopes in space.

Keywords: Exoplanets, coronagraph, starshade, high contrast, starlight suppression

1. INTRODUCTION

The first planets beyond our solar system were found almost a quarter of a century ago. Since that time, over 3000 exoplanets and a number of exoplanetary systems have been detected primarily by indirect methods including radial velocity[1], microlensing[2] and transit photometry[3] techniques. Many of these detections, including a number Earth and super-Earth sized planets were made by NASA's Kepler/K2 Mission[4] using the transit photometry technique.

Since it is now understood that exoplanets are common in the galaxy, the scientific emphasis is rapidly shifting away from simple detection of new exoplanets to direct imaging and spectroscopic characterization of these new worlds and their atmospheres. Some low-resolution spectral data on exoplanet atmospheres has been collected with the Hubble and Spitzer Space Telescopes[5,6] using the transit spectroscopy technique and more is expected from the James Webb Space Telescope (JWST)[7]. In addition, the JWST NIRCAM instrument[8] will also carry a moderate contrast coronagraph potentially capable of imaging large exoplanets and debris disks. More detailed and comprehensive exoplanet characterization leading to assessment of habitability, or indeed detection of life, will require observations that achieve higher contrast and improved spectral resolution and sensitivity.

Toward this end, NASA has made a long-term investment in the Exoplanet Exploration Program (ExEP). NASA and others are currently studying a wide range of exoplanet direct imaging and characterization mission concepts in preparation for the 2020 Astronomy and Astrophysics Decadal Survey. NASA is also aggressively pursuing maturation of several high contrast imaging and starlight suppression technologies which utilize specially shaped precision optical elements, embodied in either a coronagraph or a starshade to block the light from the parent star while controlling scattering and diffraction. These technologies are enabling for direct imaging and spectroscopic study of the orbiting exoplanets with space telescopes. Much of this technology is rapidly moving from the development phase to the design

*daniel.r.coulter@jpl.nasa.gov; phone: 818-354-3638

and engineering phase although significant challenges still exist particularly for the most challenging science objectives such as imaging and characterizing exo-Earths. In this paper we discuss the status of these technologies as well as prospects and projected performance for future exoplanet direct imaging and characterization missions utilizing these techniques.

2. CURRENT AND POTENTIAL FUTURE NASA EXOPLANET MISSIONS

2.1 Ongoing NASA Activities

The current NASA ExEP portfolio[9] includes the Kepler/K2 mission, exoplanet studies with the Hubble and Spitzer Space Telescopes, the ground-based Large Binocular Telescope Interferometer, the recently started NN-EXPLORE high precision radial velocity instrument development effort, and the Exoplanet Exploration Technology Program. Looking forward, the TESS mission[10], JWST[7], as well as WFIRST[11] will continue to open new windows on this exciting field. The WFIRST mission will include a dedicated coronagraph instrument (CGI)[12] capable of directly imaging ~Neptune-sized exoplanets and a microlensing[13] capability to further the exoplanet census. In addition, NASA has recently decided to make WFIRST starshade-compatible, and initiated a Starshade Technology Program with the idea of possibly flying a separate, probe class, starshade rendezvous mission with WFIRST once it is on orbit and operating. Finally, the ExEP is facilitating and overseeing a number of community-led exoplanet mission studies ranging from large flagship class missions to probe class missions as described below. The common thread in these exciting exoplanet mission studies is a reliance on high contrast imaging and starlight suppression techniques.

2.2 Large Exoplanet Mission Studies

NASA has commissioned four large mission studies in preparation for the 2020 Decadal Survey including two with significant exoplanet science components, which are discussed below. The National Research Council conducts the survey responding to a charter set by NASA and the NSF. The survey is extremely important in guiding NASA's mission strategy as evidenced by the fact that Chandra, Spitzer, JWST and WFIRST all received top recommendations from their respective Decadal Surveys. One of the key roles of the 2020 Decadal Survey will be to prioritize large missions to follow JWST. Science and technology definition teams (STDT's) have been formed for the missions and NASA Centers assigned responsibility for leading each study. While specific center assignments have been made, the study teams as well as the STDT's are populated from across the community.

2.2.1 LUVOIR - Large UV Optical IR Surveyor

The Large UV/Optical/IR Surveyor Mission (LUVOIR) [14] is a concept for a highly capable, multi-wavelength general-purpose space observatory in the 8-16 m range with ambitious science goals. This mission would enable a great leap forward in a broad range of astrophysics, from the epoch of reionization, through galaxy formation and evolution, to star and planet formation. LUVOIR will also carry a coronagraph instrument for directly imaging and characterizing a wide range of exoplanets, including exo-Earths that might be habitable - or even inhabited. The LUVOIR study is led by the Goddard Space Flight Center.

2.2.2 HabEx - Habitable Exoplanet Imaging Mission

The Habitable Exoplanet Imaging Mission (HabEx)[15] is a concept for an optical/infrared exoplanet space observatory in the 4-8 m range optimized to, for the first time, directly image exo-Earths, and characterize their atmospheric content. By measuring the spectra of these planets, HabEx will search for signatures of habitability such as water, and be sensitive to gases in the atmosphere such as oxygen or ozone, possibly indicative of biological activity. HabEx may utilize a coronagraph, a starshade or both. In addition to the search for life on exo-Earths, HabEx will characterize a significant number of larger exoplanets and exoplanetary systems and enable a broad range of general astrophysics. The Jet Propulsion Laboratory is leading the HabEx study.

2.3 Probe Class Mission Studies

In addition to the large mission studies, there is also interest in "probe class" missions for exoplanet science. Probe class

missions are typically characterized as those costing in the ~$0.5B-$1.0B range. NASA recently commissioned two probe class exoplanet mission concept studies, the Exoplanet-Coronagraph Probe (Exo-C)[16] and Exoplanet-Starshade Probe (Exo-S)[17], which were completed by community led STDTs in 2015. The 2020 Decadal Survey could consider and recommend one of these missions for development. Alternatively, they could recommend initiation of a new competed Astrophysics Probe Mission line (comparable to New Frontiers line in NASA's Planetary program). In preparation for such a potential outcome, the NASA SMD Astrophysics Division is considering pursuing additional probe studies. One option would involve issuing a solicitation through ROSES for Astrophysics Probe mission concept proposals. Conceptually, multiple proposals, representing a wide range of astrophysics science, could be selected for one-year studies. In the case of exoplanet science, additional probe mission options could include a Starshade Rendezvous mission for WFIRST, a transit characterization mission, an astrometry mission or even an interferometry mission. If the Decadal Survey did recommend creation of a probe mission line for Astrophysics, they would have the option of recommending NASA conduct further in-depth study of several of these probe mission concepts leading ultimately to a downselect for one or more probe missions for development and flight[18].

3. CHALLENGES OF DIRECT IMAGING, ASSESSING HABITABILITY AND DETECTING LIFE

The major challenges of direct imaging of exoplanets, thus enabling spectral characterization necessary for assessment of habitability and search for life, are twofold. First, the planets are typically 1-10 billion times fainter in reflected light than their parent stars and secondly, their angular separation from their parent star is very small, on the order of 0.1 arcsec or less. The Kepler mission results have shown that planets likely to be rocky, and thus interesting targets, are apparently abundant in the galaxy[19]. In the Habitable Zones of sun-like stars where life as we know it could exist, such small, rocky, potentially Earth-like, planets will present as ~10^{-10} contrast sources relative to their star, and their detection will require instrumental contrast stability exceeding that. As shown in Fig. 1, imaging at these contrast levels

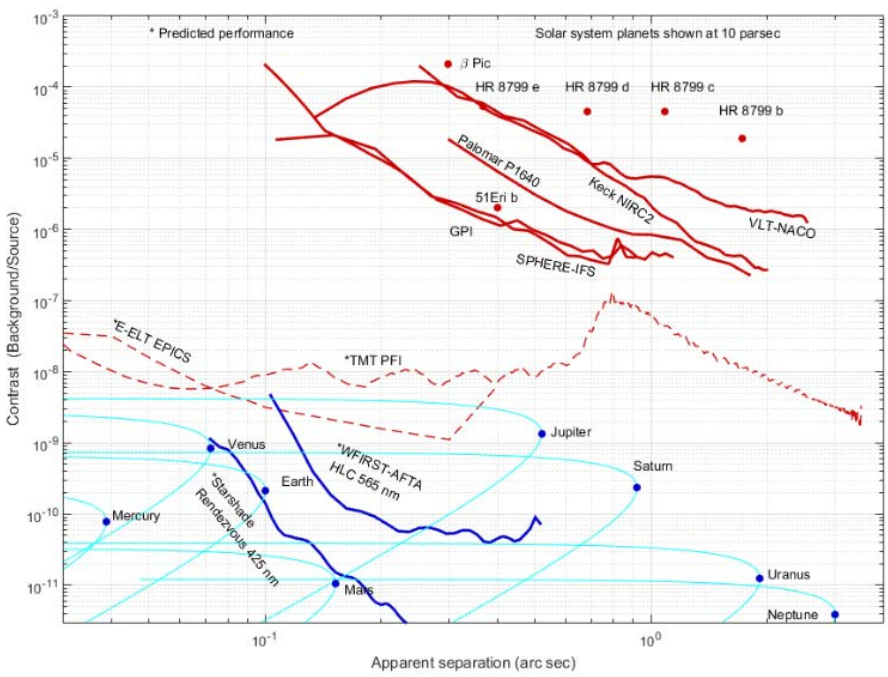

Figure 1: Contrast ratio versus apparent angular separation. The filled red circles indicate extant direct imaging of young, self-luminous gas giants imaged in the near infrared by ground-based telescopes. The filled blue circles represent the planets of the Solar System placed 10 pc away, for reference. The solid red curves are typical performance in the near-infrared of existing imaging instruments; the dashed red curves are the predicted performance of future coronagraphs on ground-based observatories. The predicted WFIRST-CoronaGraph Instrument (CGI) curve is at 565 nm and includes a factor of 10 contrast improvement from expected post-data processing gains. The predicted Starshade curve from the Exo-S study assumes a 34-m-diameter starshade flying 49,500 km away from the WFIRST telescope at 425 nm. Contrast is based on a 5-sigma level; no post-processing contrast reduction was assumed for it. The starshade curve's profile is provisional pending further community investigation. Adapted from Mawet et al. 2012[20].

will not be possible from the ground even with future extremely large telescopes equipped with high-performance adaptive optics systems[20]. The highly stable space environment offers the best prospect for directly imaging Earth-like exoplanets at the needed contrast levels. Imaging detection would be followed by moderate-to-high resolution spectroscopy of the exoplanet's reflected light to search for biosignatures such as molecular oxygen, water vapor, ozone, methane in chemical disequilibrium with oxygen, and carbon dioxide [21]. In the case where the exoplanet's orbit has not been characterized by precursor observations the problem becomes even more challenging. In that case, the imaging mission would first need to determine its orbit using multi-epoch observations in order to determine the exoplanet's location relative to the circumstellar habitable zone prior to detailed spectroscopic characterization.

4. OVERVIEW OF HIGH CONTRAST IMAGING TECHNIQUES

4.1 Introduction

NASA is currently pursuing development of two complementary approaches to achieving the high levels of starlight suppression and contrast required for exoplanet imaging and characterization. *Internal coronagraphs* use specially shaped opaque masks or pupil remapping optics to block starlight and control diffraction along with deformable mirrors (DMs) to compensate for wavefront imperfections in combination with a telescope all located on a single spacecraft. These coronagraphic components are small compared to the size of a telescope, and the elements can be rigidly mounted in a compartment behind the telescope optics. There are several classes of internal coronagraphs, which are currently candidates for exoplanet imaging and characterization. Because internal coronagraphs require only a single spacecraft, they have the advantage of being able to quickly point to multiple targets over a large region of the sky, facilitating multiple-observations to determine orbits and disambiguate background objects. They have the disadvantage of imposing stringent precision and stability requirements on the observatory and optics. Also, broadband observations are challenging with internal coronagraphs. *External coronagraphs* use a large specially shaped diffracting screen to block the starlight and control diffraction called a starshade located in space between the target star/exoplanet system and a rather ordinary telescope. When pointed at a star, this combination produces a dark shadow at the location of the telescope covering its collecting area. The starshade must be located on a second spacecraft, far enough away from the telescope so that an exoplanet to be imaged will lie outside the edge of the shadow. Typically the starshade, an opaque solid disk with petal-like scalloping of the edge, is many times the diameter of the telescope aperture and is located tens of thousands of km from the telescope. The two spacecraft holding the starshade and the telescope must be controlled along the line of sight to maintain alignment but the requirements are surprisingly modest as discussed in the next section. External coronagraphs have the advantage of shielding the telescope from starlight so that no special precision and stability requirements are imposed on the optics. Further, the starshade shape requirements and line-of-sight control are within current capabilities and broadband observations (e.g. >50% bandpass) can be achieved. But starshades typically require several days or longer to retarget, they have more restrictive solar avoidance angles than coronagraphs, and their lifetimes are limited by their fuel supply.

4.2 Internal Coronagraphs

Stellar coronagraphs are instruments designed to suppress the veiling glare of starlight due to diffraction and optical imperfections including aberrations, dust, scratches, coating pinholes, etc. Several different coronagraph designs have

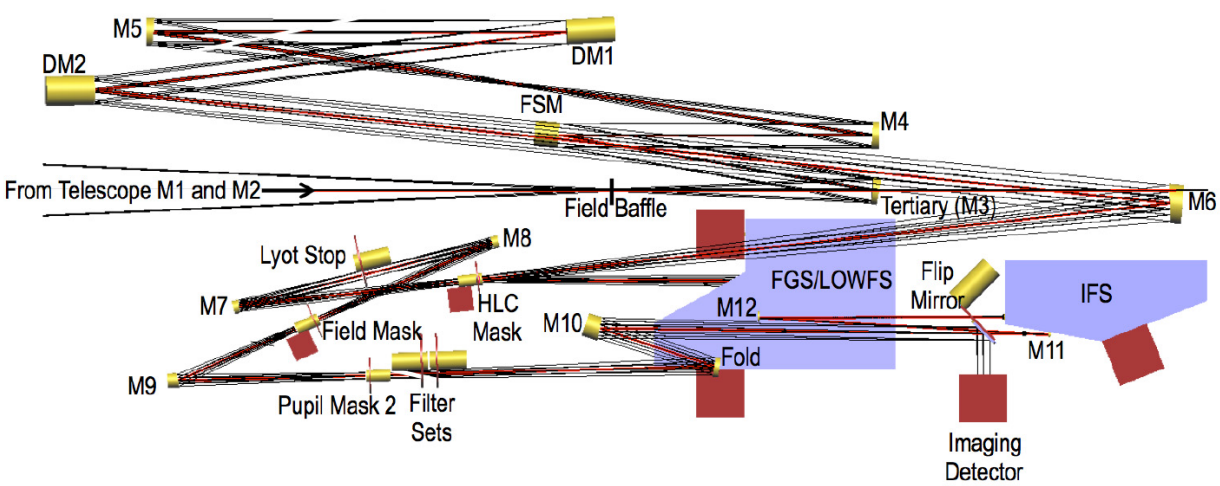

Figure 2. Layout of the Exo-C coronagraph. Coronagraphs have a pair of DMs, an FSM, and intermediate pupil and image planes were diffraction-control masks are placed. The output beam is fed to either an imaging detector an integral field spectrometer. A hybrid Lyot Coronagraph is shown. A similar layout is used for the shaped pupil and PIAA coronagraphs.

been described in the literature[22,23,24,25,26] and all rely on DMs to control critical spatial frequencies in the wavefront, and sets of masks or specially shaped optics to control diffraction, or interferometric nulling[27]. Figure 2 shows a typical instrument layout[16], in this case the EXO-C coronagraph. The overall complexity of the optical train is driven by the need to form pupil planes where DMs, Fast Steering Mirrors (FSMs), and Lyot-mask planes are positioned, as well as image planes where diffraction control masks and field stops are placed. Additional intermediate planes may be used for amplitude control using DMs[28]. Typically the image plane f/# is about 20 and the pupil planes are several cm in diameter to accommodate accuracy requirements on mask features[29,30]. Behind the coronagraph, a direct imager and an Integral Field Spectrograph (IFS)[31] perform spectrophotometric measurements and spectroscopy, respectively, typically in optical bands as wide as 10-20%. Wavefront sensing and control algorithms are central to the operation of coronagraphs. The JPL High Contrast Imaging Testbed (HCIT)[32] has successfully utilized an image plane diversity sensing approach with the Electric Field Conjugation algorithm to achieve high contrast results[33] though related approaches such as stroke minimization have also proved successful[34]. The design of coronagraphs is considerably more challenging for segmented and on-axis apertures. Diffracting edges must be either masked off, thereby reducing throughput, or effectively smoothed out using diffraction control with DMs[35]. The size of the central obscuration is typically the limiting factor and plays a major role in the design of the WFIRST coronagraphs[24,36].

4.3 External Coronagraphs

Starshades are conceptually simple – a screen far from the telescope is positioned along the line of sight to the target star and blocks the starlight. A planet orbiting the star appears to the side of the starshade so that its light is not blocked. As with coronagraphs, the major challenges are suppressing diffraction and scatter. The flower-like shape of the starshade is designed to suppress the "Spot of Arago" that would appear on axis if the shade were a simple circular disk. The petals act as an apodizer in what amounts to a pin-speck camera, forming a shadow that is up to 11 orders of magnitude darker than the unattenuated starlight. Originally conceived by Lyman Spitzer, designs evolved over the years leading to a 'practical' design by Web Cash[37]. Optimization of the petals allows for accommodation of engineering constraints such as petal tip length and width, as well as tuning of the performance for specific optical bands and telescopes. A starshade with a 34-m tip-to-tip diameter at a distance of about 34,000 km from the telescope, as shown in Figure 3, achieves an inner working angle of 100 milliarcsec in visible light, enabling it to search for Earth-like exoplanets[17].

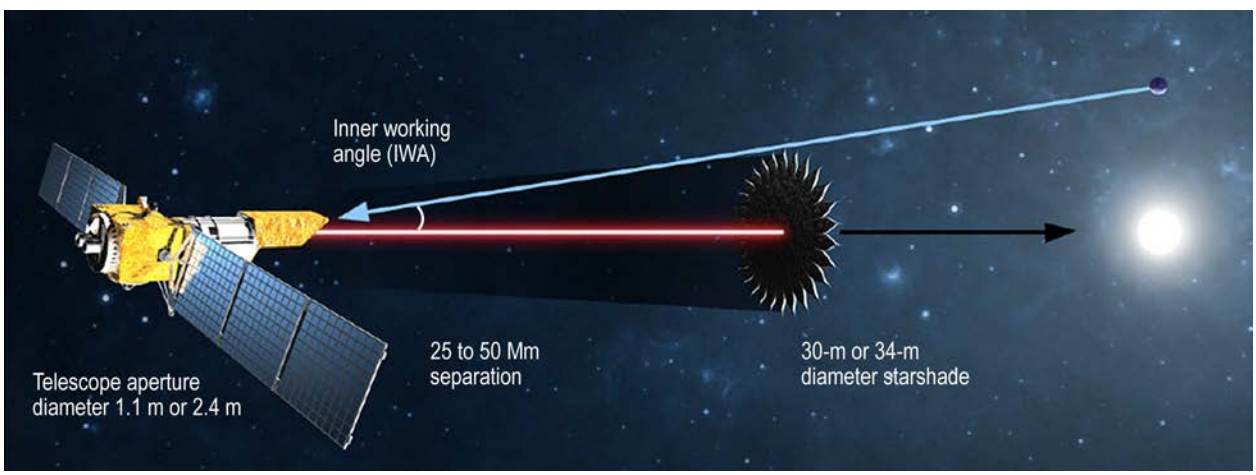

Figure 3 Starshade concept from the Exo-S report[17].

Typical requirements on the shape of the starshade are deployment to 0.5 mm, and petal shape accuracy to 100 um[38], both of which have been achieved in the laboratory[39,40]. The other key requirement is that the telescope must be positioned within the shadow, which is designed to allow +/- 1m lateral and +/- 250km longitudinal motion. Because the starshade is designed to work over a finite or semi-infinite band, typically 30-50%, diffracted light from outside the band serves as a bright, self-referencing source for the nanometric bearing sensing problem[41]. While the starshade shape must be accurate enough to provide a deep shadow, sunlight glinting from the edge adds an additional requirement for the edges to scatter a minimal amount of light through a combination of edge sharpness and low reflectivity. Edge materials are under test and being analyzed in a dedicated scatterometer[42]. Retargeting involves turning the starshade

to point the thrusters in the appropriate direction and thrusting for typically 7-14 days until the starshade approaches the desired position. A beacon on the starshade is observed by the telescope and compared to the position of the star while fine thrusters perform the final positioning. Studies have shown that enough fuel can be flown to support 5 or more years of observations[43].

5. CURRENT NASA STARLIGHT SUPPRESSION TECHNOLOGY PROGRAMS

5.1 Introduction

Since 2009 NASA has supported an annual Strategic Astrophysics Technology (SAT) proposal opportunity entitled "Technology Development for Exoplanet Missions" (TDEM). More than two dozen small projects have been funded in areas of starlight suppression, wavefront sensing and control, and other related technologies that directly support spacebased exoplanet direct imaging and characterization. Proposers have had access to the infrastructure of the HCIT for coronagraph performance demonstrations in a space-like environment. The peer-reviewed TDEM program, through awards selected by NASA HQ has advanced the technical readiness level of several coronagraph and starshade technologies through broad community participation, complementing directed investments made by NASA HQ and the Ames, Goddard, and JPL Field Centers. In order to achieve specific technology goals in time for the 2020 Decadal Survey, by 2016 NASA decided to focus its exoplanet technology efforts in two large projects. These are detailed below. Going forward, the TDEM program will continue to provide an opportunity for new small projects conceived by the community but at a reduced funding level relative to recent years.

5.2 WFIRST CGI Project

For internal coronagraphy development, the focus of NASA technology efforts is now on the CGI that NASA plans to fly on the Wide Field Infrared Survey Telescope (WFIRST) in the mid-2020s[44]. WFIRST-CGI will be the first coronagraph to fly in space using active wavefront control to improve contrast. Although hampered by the complex obscuration pattern of the WFIRST telescope, and classified as a technology demonstration, CGI is still expected to be the first science instrument to surpass 10^{-8} raw contrast at an inner working angle of 3 λ/D. This will enable the mission to take spectra of medium to large exoplanets in reflected starlight [45]. WFIRST-CGI features a hybrid Lyot coronagraph for searches and initial exoplanet detections and imaging, paired with a reflective shaped pupil coronagraph for spectroscopy once the targets are found. Nine technology milestones have been defined against which technical progress on CGI is being measured. To date the desired contrast has been demonstrated for both coronagraph types in 10% bandwidth light. Three milestones remain to be achieved in 2016: 1) A demonstration of a prototype backend spectrograph, including suitably low levels of detector noise; 2) repeating laboratory contrast demonstrations in the presence of dynamic pointing and wavefront disturbances; and 3) the first experimental tests of a backup coronagraph architecture known as PIAA-CMC[46].

5.3 Starshade Technology Project

The Exo-S Probe mission study considered the possibility of flying a starshade in combination with the either a 1.1m space telescope or, the 2.4m WFIRST telescope at the Sun-Earth L2 point. Such a mission has the potential to search the habitable zones of a few dozen nearby stars and detect a few Earth-sized planets, if they are present and levels of exozodiacal light are low[47]. The prospect of detecting even a few Earth analogs as a part of the WFIRST mission, rather than waiting for a large new exoplanet telescope in the 2030s, is intriguing but needs to be evaluated versus other possible projects by the 2020 Decadal Survey. To ensure that a viable option is developed in time for Decadal consideration, the NASA Exoplanet Exploration Program has recently formed a Starshade Technology Project to advance critical technologies on the needed timescale and define the criteria for mission technical readiness.

6. CORONAGRAPH TECHNOLOGY STATUS AND GAPS

6.1 Wavefront Control

Precision wavefront control is the key enabling technology for high contrast coronagraphic imaging. It is impractical to polish a large optic to the smoothness required to directly detect exoplanets. Instead, DMs are used to actively correct the telescope mid-spatial frequency wavefront to the very high accuracy of λ/1,000. In a space environment these corrections are expected to be highly stable on timescales of days, unlike the 10 ms timescales typical for groundbased adaptive optics. With complex pupils like that for the WFIRST mission wavefront control has been used to achieve 10^{-8} contrast in 10% bandwidths (Figure 4), and 10^{-9} contrast in 20% bandwidth for unobscured pupils. The demonstrated contrast performance is still an order of magnitude away from the 10^{-10} requirement for exo-Earth imaging, and has only been shown in a stable environment without the contrast-degrading effects of telescope pointing jitter, focus drifts, or other low-order wavefront variations. Wavefront instabilities will need to be sensed and controlled on timescales of kHz (pointing jitter), 0.01-1 Hz (telescope focus and alignment), and 1-10 mHz (mid-spatial frequency errors on the telescope primary) through the combined use of a dedicated low-order wavefront sensor and the science camera. A dynamic testbed including system-level wavefront disturbances input to the coronagraph will be essential for demonstrating flight readiness. WFIRST CGI is setting up the first such testbed and is also investigating operational scenarios for precision wavefront control on-orbit. Wavefront control experiments to achieve high contrast on segmented telescope pupils have yet to be done and will be crucial for the viability of large exoplanet telescope mission concepts.

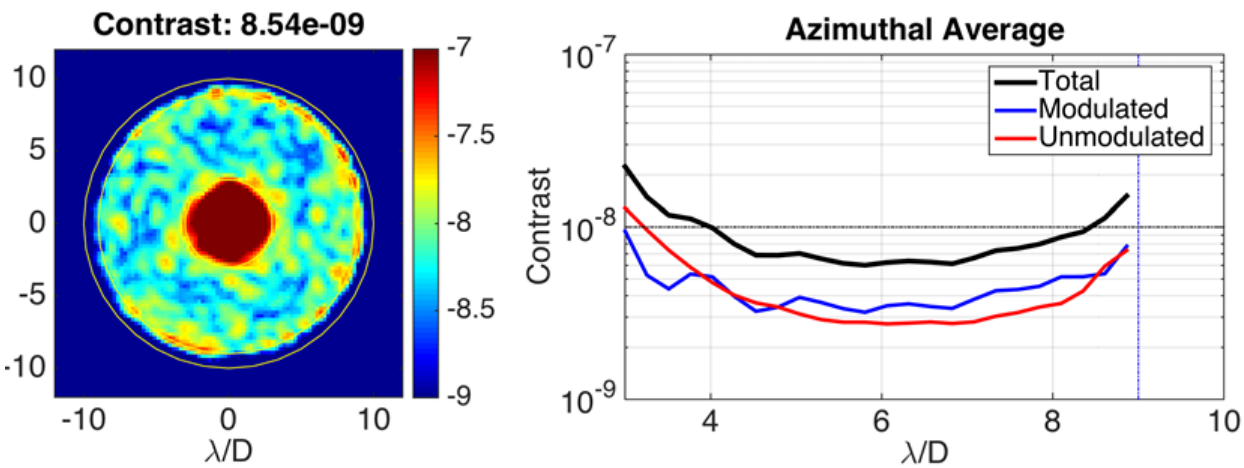

Figure 4: (Left) Focal-plane image from the WFIRST HLC testbed in HCIT-2 at JPL. (Right) Contrast curve achieved mean contrast of 8.5×10^{-9} at 10% broadband centered at 550 nm across a 3–9 λ/D dark hole (WFIRST; Milestone #5). The 10% bandwidth was achieved using five 2% bands averaged together; calibration uncertainty is ±2%. [48].

6.2 Deformable Mirrors

DMs are critical components for both coronagraph starlight suppression and contrast stability. High-contrast stellar coronagraphs depend on deformable mirrors to modulate and remove the residual starlight in the region of interest creating "dark hole" control regions. In the process, the DMs can compensate for wavefront errors due to the imperfections of the telescope and coronagraph optics. The largest continuous face sheet DMs currently available have a 64x64 actuator format; WFIRST-CGI plans the use of 48x48 DMs[49]. 4m class telescopes will require DMs in formats of 96x96, and 10m class telescopes may need to go as large as 192x192. Current Northrup Grumman Xinetics devices have a 1mm actuator pitch; a smaller pitch would be advantageous when going to larger formats. The DM size requirement is driven by a combination of the desired high contrast field of view, specified by Nλ/2D for N actuators across the pupil of a telescope with diameter D; and the complexity of the telescope pupil, which can require higher actuator counts to control the diffraction pattern with reasonable throughput. WFIRST-CGI is advancing DM flight readiness by improving the driving electronics and actuator connectors, and by testing the devices in flight-like thermal, dynamic, and radiation environments. Significant future investments will be required to develop the larger format DMs needed for a flagship exoplanet direct imaging mission.

6.3 Coronagraphs for Diffraction Control

Several options are available to suppress stellar diffraction to the levels needed to image exo-Earths. A Lyot coronagraph hybridized (HLC) with a phase mask has achieved the best bandwidth-contrast performance thus far in laboratory demonstrations[50], but with only modest throughput even for unobscured pupils. Shaped pupil coronagraphs (SPC) appear to have comparable contrast performance, are more adaptable to complex apertures, but suffer from lower throughput and a more limited instantaneous field of view[51]. Beam-shaping optics offering high throughput are the attractive aspects of the Phase-Induced Amplitude Apodization (PIAA) coronagraph. PIAA's inner working angle performance exceeds that of the hybrid Lyot or shaped pupil coronagraphs, but its bandwidth-contrast performance to date is not as good as shown by the HLC[52]. The Vector Vortex coronagraph is a focal plane phase mask with demonstrated performance similar to PIAA's but with throughput intermediate between that of HLC and PIAA[26]. For the case of segmented primary mirrors, there are no laboratory performance demonstrations to date at contrast levels relevant to exo-Earths direct imaging. Computational models suggest three approaches may be favorable: 1) Interferometric nulling of the on-axis starlight with a copy of the input beam shifted in phase by 180 degrees. Visible Nuller Coronagraph (VNC) demonstrations have achieved good contrast results but only in narrow bandpasses, very small fields of view, and without transmitting off-axis planet light[27]. The TDEM Program has funded further work to improve on this performance using a segmented primary mirror. 2) A Complex Mask Coronagraph (CMC) in the focal plane combined with weak PIAA beamshaping optics[46]. WFIRST-CGI is sponsoring this effort as its backup coronagraph architecture. A phase mask has been fabricated and will be tested for the first time in late 2016. 3) An Apodized Pupil Lyot Coronagraph (APLC) relying heavily on DM control authority to correct the complex diffraction pattern of a segmented primary mirror[53]. Amongst all these choices, mission designers and technology decision-makers should recognize that the choice of telescope pupil (clear aperture, obscured, segmented), required inner working angle, and achievable telescope stability are the primary determinants of which coronagraph to select for flight. Pending these architecture decisions, a broad-based program of coronagraph technology investment is needed to assure that the right options will be available to support a coronagraph downselect decision for the exo-Earth flagship mission in the mid-2020s.

6.4 Telescope Stability

Thermal stability and control is a key challenge for telescopes to be used with internal coronagraphs. Any future large space telescope mission will probably orbit the thermally stable Earth-Sun L2 Lagrange point, but even so there will still be thermal load variations as a function of pointing angle relative to the Sun. Exoplanet contrast requirements dictate a system stability requirement of 10 pm at low and mid spatial frequencies across the aperture per wavefront control time step. Thermal control depends on the material and architecture. Ultra-Low Expansion (ULE) glass has a low coefficient of thermal expansion (CTE), which offers good passive thermal stability and could provide the required stability with precise thermal control. Silicon carbide has 100 times the CTE of glass, which makes it more responsive than glass to precision thermal control but less stable overall. Dense mirror actuation could mitigate dimensional changes. Multiple mirror material/architecture combinations exist with the potential to meet thermal stability requirements, but they have not yet been demonstrated at the required performance levels. No previous space telescope has ever required < 10 pm wavefront stability. Historically, space telescopes use passive thermal control: JWST's telescope is in a Sunshade shadow. HST's telescope is in a heated tube. And again, while not designed to meet the requirements of a UVOIR exoplanet science mission, JWST is predicted to have a 31 nm rms WFE response to a worst-case thermal slew of 0.22 K and take 14 days to passively achieve < 10 pm per 10 min stability. A strong new effort is needed to assemble the lessons of telescope stability learned by the HST, Kepler, and Gaia missions; to assure that WFIRST is properly instrumented to teach us additional lessons on how to meet high contrast stability requirements; and to verify integrated modeling predictions of telescope mechanical stability at the levels relevant to exo-Earth direct imaging.

6.5 Post Processing

Currently demonstrated *raw* contrast for the hybrid lyot and shaped pupil coronagraphs in the HCIT testbeds at JPL is ~10^{-8} at 50-100 mas inner working angle. Further gains in contrast are necessary for both the CGI and future higher performance exoplanet observatories. Some of these gains can be realized through further improvement of the hardware but it is believed that significantly more may be achieved with state-of-the-art post-processing of the raw instrumental data. Two differential imaging techniques are currently being investigated in detailed simulations and on the HCIT

testbed. One uses a reference star and the other uses telescope rolls. In the former case, referred to as reference differential imaging (RDI), the telescope is pointed at a reference star, and the coronagraphic dark hole is created and stabilized. The telescope is then slewed to the target star (nearby in angle space to maintain approximately the same thermal condition on the telescope) and the raw imaging data are collected. During the science target observation the dark hole and its speckle field is maintained actively by using the low order wavefront sensor information. The reference and target data sets are then differenced, removing most of the residual speckles revealing any faint exoplanets that might exist. In the latter case, no reference star is used, rather the telescope is pointed at the target star, the dark hole is created and data are collected. The telescope is then rolled by a small angle of ~10-30 degrees (again to maintain approximately the same thermal condition on the telescope), and the dark hole is maintained as before. In detector space, the residual speckles move with the role while any faint exoplanets do not and are revealed after differencing the data sets. This process is referred to as angular differential imaging (ADI). Using both ADI and RDI in concert may provide further improvement. High fidelity simulation of entire observing sequences show the potential to achieve at least an order of magnitude improvement in contrast using these techniques resulting in a final contrast performance for imaging of ~10^{-9} at 50-100 mas inner working angle. Validation of these simulations and development of detailed operational sequences will be performed in the near future on the HCIT. Further development of post-processing techniques will be required to analyze IFS spectroscopic data.

7. STARSHADE TECHNOLOGY STATUS AND GAPS

7.1 Optical Performance Demonstration and Model Validation

The contrast performance of a starshade is related to its Fresnel number $F= R^2/D\lambda$, where R is the starshade radius, D is the telescope-starshade separation, and λ is the operating wavelength. For 10^{-10} contrast with a flight-scale starshade, Fresnel numbers of ≤ 20 are needed across a broadband optical bandpass. For subscale tests with starshades as small as 10 cm, the required starshade-telescope separation distances are ~0.4 km; full scale optical tests are out of the question. Even subscale performance demonstrations must be done in long tunnels or in open air such as a flat desert lakebed. Such tests aim at contrast performance consistent with imaging an exo-Earth, and can also be used to validate the optical models upon which full-scale shape tolerances are based. These mechanical tolerances can then be verified on a full-scale starshade petal.

Several experiments over the last decade demonstrate the viability of creating a dark shadow with a starshade to contrasts better than 10^{-10} just outside the petal edge. They include lab demonstrations at the University of Colorado [54], Northrop-Grumman[55], and Princeton University[56]. Northrop-Grumman has also conducted larger scale field tests on a dry lakebed[57], and night-time tests using the siderostat of the McMath Pierce solar observatory on astronomical objects. Each of these experiments has been limited in contrast performance by one or more effects including airborne dust, diffraction off the starshade support struts, starshade geometric imperfections, or the use of near-field light sources. Lakebed tests of a 58cm starshade using LED sources over a 1 km optical path achieved 10^{-9} contrast at 51 arcsec separation and a relatively large Fresnel number of 210. While not representative of the flight case, these tests allowed the starshade diffraction performance to be compared with optical models. Differences between the model predictions of three groups were revealed and later reconciled, giving confidence going forward in future design efforts. The first demonstration to be conducted at a flight-like Fresnel number (<20) is planned for fall 2016. A 78-m starshade tunnel testbed is nearing completion at Princeton University. It addresses many of the limitations identified above to hopefully yield the darkest shadow produced by a starshade to date.

7.2 Solar Glint

A starshade must always fly on the sunward hemisphere of the sky, as seen from the telescope that opeates within its shadow. This condition is necessary so that sunlight does not illuminate the front face of the starshade and produce a source brighter than the exoplanet host star being shaded. A secondary but still significant problem of scattered sunlight can arise if the starshade petals are too thick or their edges are too rough. An opaque membrane material is needed that can be integrated to the petal's structural edge to (1) meet and maintain precision in-plane shape requirements after deployment, and (2) limit the solar glint to 10^{-10} contrast at the petal edges. Analyses in the Exo-S probe study[17] show that the petal edge should be sharply beveled ($\leq$ 1 μm radius) and smooth ($\leq$ 20 μm rms). The material should also have little thermal deformation and be able to accommodate bending strain of the petal when stowed for launch. JPL,

Northrop Grumman, and Princeton are pursuing machined graphite and coated metals as potential materials, including laboratory characterization of the edge scatter. A complication to be investigated is the potential for electrostatic accumulation of dust at the sharp petal edges, which would increase the scatter.

7.3 Precision Deployable Structures

Starshade petals must be stowed for launch and then deployed without any mechanical contacts with the petal edges. The Exo-S starshade mechanical architecture stows the petals for launch in a very small volume by wrapping, or furling, them around a central hub (left panel of Figure 5). They unfurl quasi-staticly by releasing their stored strain energy. Computer-simulated petal releases conducted by Roccor Inc.[58] show unstable motion and physical contact between the unfurled petals. Northrop Grumman's deployment architecture from the New Worlds Observer Study [59], based in part on non-NASA heritage, relies on simultaneous telescopic booms to deploy both the inner disk and the petals—one boom per petal (right panel of the figure) – and may be less susceptible to edge contact. Elimination of the edge contact risk requires a demonstration of petal deployment. There is no apparent state-of-the-art for this problem. One solution being developed by JPL and Roccor is to tension radial cords through the petal stack and then cut the cords and close the openings[58]. The interface to this mechanism is built into the current petal design. The current effort is focused on producing a full-scale Petal Unfurling Testbed that is being used to develop the mechanical solution in 2016. This unfurling mechanism concept requires additional investment to complete and there may be other architectures to deploy wrapped petals.

(5a) (5b)

Figure 5: On the left (5a) is a schematic of the JPL/Exo-S petal unfurling approach[17] compared to the Northrop Grumman New Worlds Observer deployment approach[60] on the right (5b) using simultaneous deployable telescopic booms.

7.4 Lateral Formation Flying Sensing

The telescope will see a rapid increase in unocculted starlight as it drifts away from the center of the starshade's shadow, thus there is a tight constraint on the lateral position of the starshade relative to the telescope-star line of sight. Maintaining alignment is imperative to achieving the science goals of an Earth-finding mission. Position to within about ±1 m of the telescope boresight is needed to keep the telescope within the dark shadow[17]. The benign disturbance environment at either Earth-Sun L2 or an Earth Drift-Away orbit makes the control function straightforward with conventional chemical thrusters. The challenge, however, is to sense the lateral position error to within ± 30 cm at distances of tens of thousands of kilometers. While the control requirements of formation flying at L2 may not be beyond current capabilities, the accuracy of position sensing at such large separations is unprecedented. Closing this gap requires demonstrating this capability.

8. SUMMARY AND CONCLUSIONS

NASA is planning to demonstrate coronagraphy for direct imaging and characterization of large exoplanets as part of the WFIRST mission in the mid-2020s. It is likely that the 2020 Astronomy and Astrophysics Decadal Survey will recommend that the agency proceed to develop a mission to follow WFIRST capable of directly imaging and characterizing exo-Earths, assessing habitability and searching for evidence of life. NASA is aggressively pursuing maturation of high contrast imaging and starlight suppression technologies, which will enable such missions. Much progress has been made and successful conclusion of the technology plan for the WFIRST CGI instrument is in sight. Preliminary design of this instrument is in progress. With NASA's recent decision to begin a Starshade Technology Project, coupled with significant development already underway, rapid progress for a complementary technique can also be expected. While the development status of these techniques is approaching that necessary to execute missions to study medium to large planets, much remains to be accomplished to enable definitive study of exo-Earths.

ACKNOWLEDGEMENT

The research described in this publication was carried out at the Jet Propulsion Laboratory, California Institute of Technology, under a contract with the National Aeronautics and Space Administration.

REFERENCES

Fischer, D. A., et al. "State of the Field: Extreme Precision Radial Velocities", Publications of the Astronomical Society of the Pacific, Vol. 128, Number 964 (2016)

[1] Giannini, E., Lunine, J., "Microlensing detection of extrasolar planets", Reports on Progress in Physics, Vol. 76, Number 5 (2013)

[2] Charbonneau, D., Brown, T., Burrows, A., Laughlin, G., "When Extrasolar Planets Transit their Parent Stars", in Protostars & Planets V, ed. B. Reipurth, D. Jewitt, K. Keil (Tucson: University of Arizona Press) (2006)

[3] Borucki, W. J., "KEPLER Mission: development and overview", Reports on Progress in Physics, Vol. 79, Number 3 (2016)

[4] Seager, S., Deming, D., 2010, Annual Reviews of Astronomy and Astrophysics , 48, 631. "Exoplanet Atmospheres"

[5] Stevenson, K.B., Bean, J.L., Seifahrt, A., Désert, J-M., Madhusudhan, N., Bergmann, M., Kreidberg, L., Homeier D., 2014, Astronomical Journal, 147, 161. "Transmission Spectroscopy of the Hot Jupiter WASP-12b from 0.7 to 5 μm"

[6] Beichman, C., et. al., "Observations of Transiting Exoplanets with the James Webb Space Telescope (JWST)" Publications of the Astronomical Society of the Pacific, Vol. 126, Number 1134 (2014)

[7] Greene, T.P., Line, M.R., Montero, C., Fortney, J., Lustig-Yeager, J., Luther, K., "Characterizing Transiting Exoplanet Atmospheres with JWST", Astrophysical Journal, 817, 17 (2015)

[8] "Exoplanet Exploration Program", https://exoplanets.nasa.gov/exep/ (2016)

[9] "TESS: Transiting Exoplanet Survey Satellite", http://tess.gsfc.nasa.gov/overview.html (2016)

[10] Content, D., Aaron, K., Abplanalp, L., Anderson, K., Capps, R., Chang, Z.,Dooley, J., Egerman, R., Goullioud, R., Kleine, D., Kruck, J., Kuan, G., Melton, M., Ruffa, J., Underhill, M.,Van Buren, D., "Wide-Field InfraRed Survey Telescope (WFIRST) 2.4-meter mission study,", Proc. SPIE 8860, UV/Optical/IR Space Telescopes and Instruments: Innovative Technologies and Concepts VI, (2013)

[11] Zhao, Feng, "WFIRST-AFTA Coronagraph Instrument Overview", Proc. of SPIE Vol. 9143, Space Telescopes and Instrumentation 2014: Optical, Infrared, and Millimeter Wave, edited by Jacobus M. Oschmann, Jr., Mark Clampin, Giovanni G. Fazio, Howard A. MacEwen, (2014)

[12] Barry, R., Kruck, J., Anderson, J., Beaulieu, J-P., Bennett, D. P., Catanzarite, J., Cheng, E., Gaudi, S., Gehrels, N., Kane, S., Lunine, J., Takahiro, S., Tanner, A., Traub, W., "The Exoplanet Microlensing Survey by the Proposed WFIRST Observatory", Proc. of SPIE Vol. 8151, Techniques and Instrumentation for Detection of Exoplanets V, edited by Stuart Shaklan (2011)

[13] "LUVOIR- Large UV/Optical/Infrared Surveyor", http://asd.gsfc.nasa.gov/luvoir/, (2016)

[14] "Habitable Exoplanet Imaging Mission (HabEx)", http://www.jpl.nasa.gov/habex/, (2016)

[15] Stapelfeldt, K., et al, Exo-C Imaging Nearby Worlds, Final Report https://exep.jpl.nasa.gov/stdt/Exo-C_Final_Report_for_Unlimited_Release_150323.pdf (2015).
[16] Seager, S., et al, Exo-S Starshade Probe-Class Exoplanet Direct Imaging Mission Concept Final Report, https://exep.jpl.nasa.gov/stdt/Exo-S_Starshade_Probe_Class_Final_Report_150312_URS250118.pdf (2015).
[17] Paul Hertz, charge to NASA Astrophysics Program Analysis Groups at the 227th Meeting of the American Astronomical Society, Kissimmee, FL January 2016
[18] Burke, C.J. et al. 2015 "Terrestrial Planet Occurrence Rates for the Kepler GK Dwarf Sample", Astrophysical Journal, Vol. 809:8 (2015)
[19] Mawet, D. et al., "Review of small-angle coronagraphic techniques in the wake of ground-based second-generation adaptive optics systems", Proc. SPIE 8442:04 (2012)
[20] Delcanton, J. et al., "From Cosmic Birth to Living Earths: The Future of UVOIR Space Astronomy", arXiv:1507.04779 (2015)
[21] Trauger, Moody, D., Gordon, B., Krist, J., Mawet, D., "Complex apodization Lyot coronagraphy for the direct imaging of exoplanet systems: design, fabrication, and laboratory demonstration," Proc. SPIE 8442, 84424Q (2012).
[22] Guyon, O., Martinache, F., Belikov, R., Soummer, R., "High performance PIAA coronagraphy with complex amplitude focal plane masks," Astrophysical Journal Supplement, Vol. 190(2), 220-232 (2010).
[23] Zimmerman, N., Eldorand Riggs, A.J., Kasdin, N.J., Carlotti, A., Vanderbei, R.J., "Shaped pupil Lyot coronagraphs: high-contrast solutions for restricted focal planes," Journal of Astronomical Telescopes, Instruments and Systems, 2(1), 011012 (2016).
[24] Soummer, R., Sivaramakrishnan, A., Pueyo, L., Oppenheimer, B.R., "Apodized Pupil Lyot Coronagraphs for Arbitrary Apertures III. Quasi-achromatic Solutions," the Astrophysical Journal, Vol. 729(2), 144 (2011).
[25] Mawet, D., Serabyn, E., Moody, D., Kern, B., Niessner, A., Kuhnert, A., Shemo, D., Chipman, R., McClain, S., Trauger, J., "Recent results of the second generation of vector vortex coronagraphs on the high-contrast imaging testbed at JPL," Proc. SPIE 8151, 81511D (2011)
[26] Lyon, R., Clampin, M., Petrone, P., Mallik, U., Madison, T., Bolcar, M.R., "High contrast vacuum nuller testbed (VNT) contrast, performance, and null control," Proc. SPIE 8442, 844208 (2012)
[27] Shaklan. S., and Green, J., "Reflectivity and optical surface height requirements in a broadband coronagraph 1. Contrast floor due to controllable spatial frequencies," Applied Optics, 45, 5143-5153 (2006).
[28] Balasubramanian, K., White, V., Yee, K., Echternach, P., Muller, R., Dickie, M., Cady, E., Mejia Prada, C., Ryan, D., Poberezhskiy, I., Kern, B., Zhou, H., Krist, J., Nemati, B., Eldorado Riggs, A.J., Zimmerman, N.T., Kasdin, N.J., "WFIRST-AFTA coronagraph shaped pupil masks: design, fabrication, and characterization," Journal of Astronomical Telescopes, Instruments and Systems, 2(1), 011005 (2016)
[29] Seo, B-J., et al, "Hybrid Lyot coronagraph for wide-field infrared survey telescope astrophysics focused telescope assets: occulter fabrication and high contrast narrow band testbed demonstration," Journal of Astronomical Telescopes, Instruments and Systems, 2(1), 011019 (2016)
[30] McElwain, M., Gong Q., Wilkins, A.N., Stapelfeldt, K.R., Woodgate, B.E., Heap, S.R., Hilton, G.M., Kruk, J.W., Perrin, M.D., Brandt, T.D., Moody, D., Trauger, J., "PISCES: an integral field spectrograph to advance high contrast imaging technologies," Proc. SPIE 8864, 88641Q (2013)
[31] Sidick, E., Shaklan, S., Krist, J., Cady, E.J., Kern, B., Balasubramanian, K, "HCIT contrast performance sensitivity studies: simulation versus experiment," Proc. SPIE 8864, 88640Q (2013)
[32] Give'On, A., "A unified formalism for high contrast imaging correction algorithms," Proc. SPIE 7440, 74400D-1 (2009)
[33] Kay, J., Pueyo, L.A., Kasdin, N.J., "Demonstration of a symmetric dark hole with a stroke-minimizing correction algorithm," Proc . SPIE 7209, 72090G (2009).
[34] Mazoyer, J., Pueyo, L., Norman, C., N'Diaye, M., van der Marel, R.P., Soummer, R., "Active compensation of aperture discontinuities for WFIRST-AFTA: analytical and numerical comparison of propagation methods and preliminary results with a WFIRST-AFTA-like pupil," Journal of Astronomical Telescopes, Instruments and Systems, 2(1), 011008 (2016)
[35] Trauger, J.T., Moody, D., Krist, J., Gordon, B., "Hybrid Lyot coronagraph for WFIRST-AFTA: coronagraph design and performance metrics," Journal of Astronomical Telescopes, Instruments and Systems, 2(1), 011013 (2016)
[36] Cash, W., "Detection of Earth-like planets around nearby stars using a petal-shaped occulter," Nature 442, 51-53 (2006)

[37] Shaklan, S., Marchen, L., Cady, E., Ames, W., Lisman, D., Martin, S.R., Thomson, M., Regehr, M., "Error Budgets for the Exoplanet Starshade (Exo-S) Probe-Class Mission Study, Proc. SPIE 9605, 96050Z (2015)
[38] Kasdin, N. J., Lisman, D., Shaklan, S., Thomson, M., Cady, E., Martin, S., Marchen, L., Vanderbi, R.J., Macintosh, B., Rudd, R.E., Savransky, D., Mikula, J., Lynch, D., "Technology demonstration of starshade manufacturing for NASA's Exoplanet Mission Program," Proc. SPIE 8442, 84420A (2012)
[39] Webb, D., Kasdin, N. J., Lisman, D., Shaklan, S., Thomson, M., Cady, E., Marks, G.W., Lo, A., "Successful starshade petal deployment tolerance verification in support of NASA's technology development for exoplanet missions," Proc. SPIE 9151, 91511P (2014)
[40] Scharf, D., Martin, S., Liebe, C., Noecker, M., Rahman, Z., Seubert, C., Purcell, G., *Precision f*ormation flying at megameter separations for exoplanet characterization," Acta Astronautica, Vol. 123, 420-434 (2016).
[41] Martin, S., Shaklan, S., Crawford, S., Lee, S-C., Khayatian, B., Hoppe, D., Cady, E., Lisman, D., "Starshade optical edge modeling, requirements and laboratory tests," Proc. SPIE 8864, 88641A (2013)
[42] Trabert, R., Shaklan, S., Lisman, P.D., Roberge, A., Turnbull, M., Domagal-Goldman, S., Stark, C., "Design Reference Missions for the Exoplanet Starshade (Exo-S) Probe Class Study, Proc. SPIE. 9605, 96050Y (2015)
[43] Spergel, D., Gehrels, N. et al. 2015 "Wide-Field InfrarRed Survey Telescope-Astrophysics Focused Telescope Assets WFIRST-AFTA 2015 Report" arXiv:1503.03757.
[44] Traub, W.A., Belikov, R., Guyon, O., Kasdin, N.J., Krist, J., Macintosh, B., Mennesson, B., Savransky, D., Shao, M., Serabyn, E., Trauger, J., "Science yield estimation for AFTA coronagraphs", Proc. SPIE 9143, 91430N (2014)
[45] Guyon, O., Hinz, P.M., Cady, E., Belikov, R., Martinache, F., "High Performance Lyot and PIAA Coronagraphy for Arbitrarily Shaped Telescope Apertures", The Astrophysical Journal 780:171 (2014)
[46] Seager, S., Turnbull, M., Sparks, W., Thomson, M., Shaklan, S., Roberge, A., Kuchner, M., Kasdin, N.J., Domegal-Goldman, S., Cash, W., Warfield, K., Lisman, D., Scharf, D., Webb, D., Trabert, R., Martin, S., Cady, E., Heneghan, C., "The Exo-S probe class starshade mission", Proc. SPIE 9605, 96050W (2015)
[47] Trauger, J., Gordon, B., Krist, J., Moody, D., "Hybrid Lyot coronagraph for WFIRST-AFTA: coronagraph design and performance metrics" Proc. SPIE 9605, 96050N (2015)
[48] Poberezhskiy, I. et al. 2014 "Technology development towards WFIRST-AFTA coronagraph" Proc. SPIE 9143
[49] Trauger, J.T. et al. 2012 "Complex apodization Lyot coronagraphy for the direct imaging of exoplanet systems: design, fabrication, and laboratory demonstration" Proc. SPIE 8442
[50] Zimmerman, N., Eldorand Riggs, A.J., Kasdin, N.J., Carlotti, A., Vanderbei, R.J., "Shaped pupil Lyot coronagraph designs for WFIRST/AFTA" Proc. SPIE 9605, 96050A (2015)
[51] Guyon, O., Kern, B., Kuhnert, A., Niessner, A., "Phase-Induced Amplitude Apodization (PIAA) Technology Development, Milestone 3, 10% Contrast Demonstration Report", JPL Document D-93064, http://exep.jpl.nasa.gov/technology/Guyon-PIAA-Milestone-3.pdf (2014)
[52] N'Diaye, M., Soummer, R., Pueyo, L., Carlotti, A., Stark, C.C., Perrin, M.D., "Apodized Pupil Lyot Coronagraphs for Arbitrary Apertures. V. Hybrid Shaped Pupil Designs for Imaging Earth-like planets with Future Space Observatories" Astrophysical Journal, Vol. 818(2), 163 (2016)
[53] Leviton, D. B., Cash, W. C., Gleason, B., Kaiser, M.J., Levine, S.A., Lo, A.S., Schindhelm, E., Shipley, A.F., "White-light demonstration of one hundred parts per billion irradiance suppression in air by new starshade occulters." Proc. SPIE 6687, 66871B (2007)
[54] Samuele, R., Varshneya, R., Johnson, T. P., Johnson, A.M.F., Glassman, T., "Progress at the starshade testbed at Northrop Grumman Aerospace Systems: comparisons with computer simulations," Proc. SPIE 7731, 773151 (2010)
[55] Sirbu, D., Kasdin, N. J., Vanderbei, R. J., "Progress on optical verification for occulter-based high contrast imaging," Proc. SPIE 8864, 8864-43 (2013)
[56] Glassman, T., Novicki, M., Richards, M., Smith, D., Warwick, S., Patterson, K., Harness, A., 2012 TDEM: "Demonstration of Starshade Starlight-Suppression Performance in the Field". Final Report http://exep.jpl.nasa.gov/files/exep/GlassmanTDEM2012_FinalReport.pdf (2015)
[57] Francis, W., Roccor, LLC, " An Outrigger Component for a Deployable Occulter System- Final Report", NASA Phase II SBIR, Number NNX14CP08C (2016)
[58] Cash, W., and the New Worlds Observer Study Team, "Astro2010 PPP RFI Response- The New Worlds Observer", *cor.gsfc.nasa.gov/copag/**rfi**/149_**newworlds**_Cash_EOS.pdf* (2010)
[59] Lo, A.S., Cash, W., Hyde, T., Polidan, R., Glassman, T., and the New Worlds Observer Study Team, "Astro2010 Technology Development White Paper- Starshade Technology Development", http://newworlds.colorado.edu/documents/Decadal/Lo_Starshades_TEC_EOS.pdf (2010)